Bloch sphere-like construction of *SU*(3) Hamiltonians using unitary integration

2009 J. Phys. A: Math. Theor. 42 425303

(http://iopscience.iop.org/1751-8121/42/42/425303)

IOP PUBLISHING JOURNAL OF PHYSICS A: MATHEMATICAL AND THEORETICAL

J. Phys. A: Math. Theor. **42** (2009) 425303 (17pp) doi:10.1088/1751-8113/42/42/425303

Bloch sphere-like construction of $SU(3)$ Hamiltonians using unitary integration

Sai Vinjanampathy and A R P Rau

Department of Physics and Astronomy, Louisiana State University, Baton Rouge, LA 70803-4001, USA

E-mail: saiv@phys.lsu.edu and arau@phys.lsu.edu

Received 3 June 2009, in final form 3 September 2009
Published 30 September 2009
Online at stacks.iop.org/JPhysA/42/425303

Abstract

The Bloch sphere is a familiar and useful geometrical picture of the time evolution of a single spin or a quantal two-level system. The analogous geometrical picture for three-level systems is presented with several applications. The relevant $SU(3)$ group and $su(3)$ algebra are eight-dimensional objects and are realized in our picture as two four-dimensional manifolds that describe the time evolution operator. The first, called the base manifold, is the counterpart of the S^2 Bloch sphere, whereas the second, called the fiber, generalizes the single $U(1)$ phase of a single spin. Now four dimensional, it breaks down further into smaller objects depending on alternative representations that we discuss. Geometrical phases are also developed and presented for specific applications. Arbitrary time-dependent couplings between three levels or between two spins (qubits) with $SU(3)$ Hamiltonians can be conveniently handled through these geometrical objects.

PACS numbers: 02.40.Yy, 02.20.Qs, 03.67.Lx, 03.65.Vf, 03.65.Fd

(Some figures in this article are in colour only in the electronic version)

1. Introduction

Three-level systems are of fundamental importance to many branches of physics. While two levels give the simplest model for the dynamics of discrete systems, three levels illustrate the role that an intermediate state can play in inducing transitions between the other two. Canonical examples of this include applications in quantum optics that use three-level atoms to control quantum-state evolution [1]. Such laser control is used, for instance, to transfer population between two states using stimulated Raman adiabatic passage (STIRAP) [2, 3] and chirped adiabatic passage (CARP) [4]. In some of these systems, the interaction of the radiation with the atom is represented as a time-dependent Hamiltonian inducing an energy

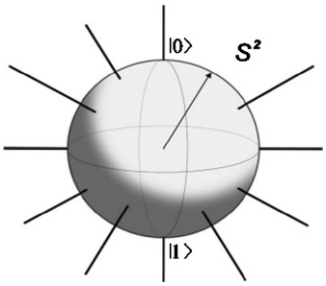

Figure 1. Bloch or Poincaré sphere representation for $SU(2)$. The base manifold is the S^2 sphere while the fiber is given by the $U(1)$ phase at each point on that sphere. Together, we have the fiber bundle $SU(2) \simeq S^2 \times U(1)$.

separation between the two states that varies with time. For a non-zero sweep rate, it can be shown that there is a finite transition probability between the states [5–7]. The study of Landau–Zener transitions in multilevel systems is of interest to understand the interplay between various level crossings [8]. Particle physics represents another example where three-level systems play a central role as, for example, the oscillations of neutrino flavor eigenstates [9].

The general Hamiltonian of a three-level system involves eight independent operators. Such a set can also naturally arise as a subgroup of higher level systems where there is some degeneracy involved. Thus, several important two-qubit problems in quantum computing and quantum information can so be written in terms of eight operators that form a subalgebra of the full 15 operators that describe two spins. The Hamiltonian describing anisotropic spin exchange is an example of one such important physical problem. While isotropic spin exchange has been explored to design two-qubit gates in quantum computing, anisotropic spin exchange has been studied as a possible impediment to two-qubit gate operations [10, 11]. Such an $SU(3)$ Hamiltonian is given by

$$\mathbf{H}(t) = J(t)(\vec{\sigma} \cdot \vec{\tau} + \vec{\beta}(t) \cdot (\vec{\sigma} \times \vec{\tau}) + \vec{\sigma} \cdot \mathbf{\Gamma}(t) \cdot \vec{\tau}), \tag{1}$$

when written in terms of a scalar, a vector and a symmetric tensor operator expressed in terms of two Pauli spins. Here, $\vec{\beta}(t)$ is the Dzyaloshinksii–Moriya vector [12, 13] and $\mathbf{\Gamma}(t)$ is the (traceless) symmetric interaction term. While the first term is the familiar Ising interaction Hamiltonian [14], the last two terms are due to the spin–orbit coupling.

Given this wide applicability, a geometrical picture of the dynamics of three-level systems can be useful. For a two-level system, the geometry of the evolution operator is well known. Any density matrix can be written as $\boldsymbol{\rho} = (I^{(2)} + \vec{n} \cdot \vec{\sigma})/2$, where $\vec{\sigma}$ are the Pauli matrices. Unitary evolution of $\boldsymbol{\rho}$ is represented as the vector $\vec{n}$ rotating on the surface of a three-dimensional unit sphere called the Bloch sphere [15]. This vector, along with a phase, accounts for the three parameters describing the time-evolution operator of a two-level system. The vector $\vec{n}$, along with the phase factor, is shown in figure 1. The vector $\vec{n}$ shown traces out the 'base manifold' and together with the global phase factor or 'fiber' at each point on that manifold is referred to as a 'fiber bundle' [16]. While the density matrix is independent of it, the complete description of the system requires this phase as well. The aim of this paper is to provide an analogous geometrical picture for a three-level system with appropriate generalizations of the base and fiber.

Some work already exists regarding the geometry of $SU(3)$. Following Wei and Norman [17], Dattoli and Torre have constructed the 'Rabi matrix' for a general $SU(3)$ unitary evolution in [18]. Mosseri and Dandoloff in [19] described the generalization of the Bloch sphere

construction of single qubits to two qubits via the Hopf fibration description. This method relies upon the homomorphism between the $SU(2)$ and $SO(3)$ groups and likewise between the $SU(4)$ and $SO(6)$ groups. In [20], the authors propose a generalized Euler angle parameterization for $SU(4)$. This decomposition is similar to the work in [21–27] into which fits our treatment of $SU(3)$ in this paper.

Another well-known choice of the (N^2-1) generators $\mathbf{s}_j$ of the $SU(N)$ group was studied in [28, 29]. Consider $\mathbf{s}_j$, chosen to be traceless and Hermitian such that $[\mathbf{s}_i, \mathbf{s}_j] = 2\mathrm{i} f_{ijk}\mathbf{s}_k$ and $\mathrm{Tr}\{\mathbf{s}_i\mathbf{s}_j\} = 2\delta_{jk}$. Here, f_{ijk} is the completely antisymmetric symbol which for a two-level system is the Levi Civita symbol ϵ_{ijk}, and a repeated index is summed over. In this basis, the Hamiltonian is written as $\mathbf{H}(t) = \Gamma_i\mathbf{s}_i$. With this choice, the Liouville–Von Neumann equation for the density matrix $\boldsymbol{\rho} = \mathbf{I}/N + S_j\mathbf{s}_j/2$ becomes $\dot{S}_i = f_{ijk}\Gamma_j S_k$. Note that for the $N = 2$ case, this is the familiar Bloch sphere representation. But, for $SU(3)$, this representation differs from that we present in two aspects. First, the 'coherence vector', whose elements are real and are given by S_j, experiences rotations in a (N^2-1)-dimensional space. For instance, for $SU(3)$, the coherence vector undergoes rotations in an eight-dimensional space. Arbitrary rotations in eight dimensions are characterized by 28 parameters. But since a three-level Hamiltonian is only characterized by eight real quantities, this means that the coherence vector is not permitted arbitrary rotations and is instead constrained. Second, the coherence vector representation does not differentiate between local and non-local operations. Our decomposition of the time-evolution operator into a diagonal and an off-diagonal term in this paper is more suited for this differentiation. Such a parameterization of the time-evolution operator in terms of local and non-local operations can be useful in understanding entanglement. The aim of this paper is to discuss the geometry of two-qubit time-evolution operators in terms of such a decomposition. The authors in [30] discuss an alternative decomposition of two-qubit states in terms of two three-vectors and a 3×3 dyadic to discuss entanglement.

A series of papers presented a systematic approach to studying N-level systems using a program of unitary integration [21–27, 31, 32]. Continuing this program, we present a complete analytical solution to the three-level problem that generalizes the Bloch sphere approach to three levels. Below, we define the fiber bundle via two different decompositions which allows us to extract the geometric phases associated with a three-level system (for a discussion on the quantum phases of two-level and three-level systems, see [33–36]). These fiber bundles are $\{SU(3)/SU(2) \times U(1)\} \times \{SU(2) \times U(1)\}$ and $\{SU(4)/[SU(2) \times SU(2)]\} \times \{SU(2) \times SU(2)\}$.

The structure of this paper is as follows. Section 2 outlines the unitary integration program to solve time-dependent operator equations. Section 3 uses this technique for the solution of a general time-dependent $SU(3)$ Hamiltonian completely analytically. Section 4 presents the geometry of the time-evolution operator for $SU(3)$ with some applications. Section 5 presents a coordinate description that is useful to define the geometric phase for three-level systems, and section 6 presents the conclusions. The appendix will present an alternative analytical solution to the three-level problem by exploiting the natural embedding of $SU(3)$ in $SU(4)$.

2. Unitary integration

Many important applications in physics involve time dependence in the Hamiltonian. For such systems, the time-evolution operator is not given by the simple exponentiation of the Hamiltonian [37]. To handle the time evolution for such Hamiltonians iteratively, 'unitary integration' was proposed in [21–24]. Earlier work with this technique is presented in [17, 29]. Later, the technique was presented as generalizing the $SU(2)$ example to solve iteratively for

the time-evolution operator $\mathbf{U}^{(N)}(t)$ of N-level systems [31, 32]. Consider the N-dimensional Hamiltonian $\mathbf{H}^{(N)}$ given by

$$\mathbf{H}^{(N)} = \begin{pmatrix} \mathbf{H}^{(N-n)} & \mathbf{V} \\ \mathbf{V}^\dagger & \mathbf{H}^{(n)} \end{pmatrix}. \tag{2}$$

The diagonal blocks are $(N-n)$- and (n)-dimensional square matrices, respectively, while $\mathbf{V}$ is an $(N-n)\times(n)$-dimensional matrix.

The evolution operator $\mathbf{U}^{(N)}(t)$ for such a $\mathbf{H}^{(N)}$ is written as a product of two operators $\mathbf{U}^{(N)}(t) = \widetilde{U}_1\widetilde{U}_2$, where

$$\begin{aligned} \widetilde{U}_1 &= \begin{pmatrix} \mathbf{I}^{(N-n)} & \mathbf{z}(t) \\ \mathbf{0}^\dagger & \mathbf{I}^{(n)} \end{pmatrix} \begin{pmatrix} \mathbf{I}^{(N-n)} & \mathbf{0} \\ \mathbf{w}^\dagger(t) & \mathbf{I}^{(n)} \end{pmatrix}, \\ \widetilde{U}_2 &= \begin{pmatrix} \widetilde{\mathbf{U}}^{(N-n)} & \mathbf{0} \\ \mathbf{0}^\dagger & \widetilde{\mathbf{U}}^{n} \end{pmatrix}. \end{aligned} \tag{3}$$

For any N, n is arbitrary with $1 \leqslant n < N$, and the tilde denotes that the matrices need not be unitary. The product of three factors parallels the product of exponentials in three Pauli matrices. Equations defining the rectangular matrices $\mathbf{z}(t)$ and $\mathbf{w}^\dagger(t)$ are developed and the problem is reduced to the two residual $(N-n)$- and (n)-dimensional evolution problems sitting as diagonal blocks of $\widetilde{U}_2$. $\mathbf{z}(t)$ and $\mathbf{w}^\dagger(t)$ are related to each other through the unitarity of $\mathbf{U}^{(N)}(t)$ [31, 32]:

$$\mathbf{z} = -\boldsymbol{\gamma}_1\mathbf{w} = -\mathbf{w}\boldsymbol{\gamma}_2, \tag{4}$$

with $\boldsymbol{\gamma}_1 = \hat{\mathbf{I}}^{(N-n)} + \mathbf{z}\cdot\mathbf{z}^\dagger$ and $\boldsymbol{\gamma}_2 = \hat{\mathbf{I}}^{(n)} + \mathbf{z}^\dagger\cdot\mathbf{z}$.

With $\mathbf{U}^{(N)}(t)$ in such a product form, the Schrödinger equation is written as

$$\begin{aligned} \mathrm{i}\dot{\widetilde{U}}_2(t) &= \mathbf{H}_{\mathtt{eff}}\widetilde{U}_2, \\ \mathbf{H}_{\mathtt{eff}} &= \widetilde{U}_1^{-1}\mathbf{H}^{(N)}\widetilde{U}_1 - \mathrm{i}\widetilde{U}_1^{-1}\dot{\widetilde{U}}_1. \end{aligned} \tag{5}$$

Here, the overdot denotes differentiation with respect to time. Since $\widetilde{U}_2$ is block diagonal, the off-diagonal blocks of equation (5) define the equation satisfied by $\mathbf{z}$

$$\mathrm{i}\dot{\mathbf{z}} = \mathbf{H}^{(N-n)}\mathbf{z} + \mathbf{V} - \mathbf{z}(\mathbf{V}^\dagger\mathbf{z} + \mathbf{H}^{(n)}). \tag{6}$$

Note that the initial condition $U^N(0) = \mathbf{I}^N$ implies that $\widetilde{U}_1(0) = \mathbf{I}^{(N-n)}$, $\widetilde{U}_2(0) = \mathbf{I}^{(n)}$ and $\mathbf{z}(0) = \mathbf{0}^{(N-n)}$. Equation (6) along with the initial condition can be solved to determine $\mathbf{z}$ and thereby $\widetilde{U}_1$ and $\mathbf{H}_{\mathtt{eff}}$ for the subsequent solution of equation (5) for $\widetilde{U}_2$. In this manner, the procedure iteratively determines $U^{(N)}(t)$.

Before discussing the geometry of the time-evolution operators for this unitary case, we briefly mention the procedure for dealing with non-Hermitian Hamiltonians. For such a non-Hermitian Hamiltonian,

$$\mathbf{H}^{(N)} = \begin{pmatrix} \widetilde{\mathbf{H}}^{(N-n)} & \mathbf{V} \\ \mathbf{Y}^\dagger & \widetilde{\mathbf{H}}^{(n)} \end{pmatrix}, \tag{7}$$

where the tilde denotes possibly non-Hermitian character, and the off-diagonal components $\mathbf{V}$ and $\mathbf{Y}$ are independent. In this case, equation (6) is replaced by

$$\mathrm{i}\dot{\mathbf{z}} = \widetilde{\mathbf{H}}^{(N-n)}\mathbf{z} + \mathbf{V} - \mathbf{z}(\mathbf{Y}^\dagger\mathbf{z} + \widetilde{\mathbf{H}}^{(n)}), \tag{8}$$

and there is a separate equation governing the evolution of $\mathbf{w}$ given by

$$\mathrm{i}\dot{\mathbf{w}}^\dagger = \mathbf{w}^\dagger(\mathbf{z}\mathbf{Y}^\dagger - \widetilde{\mathbf{H}}^{(N-n)}) + (\widetilde{\mathbf{H}}^{(n)} + \mathbf{Y}^\dagger\mathbf{z})\mathbf{w}^\dagger + \mathbf{Y}^\dagger. \tag{9}$$

The diagonal terms of the time-evolution operators are governed by

$$\mathrm{i}\dot{\widetilde{U}}_2(t) = \begin{pmatrix} \widetilde{\mathbf{H}}^{(N-n)} - \mathbf{z}\mathbf{Y}^\dagger & 0 \\ 0 & \widetilde{\mathbf{H}}^{(n)} + \mathbf{Y}^\dagger\mathbf{z} \end{pmatrix}\widetilde{U}_2. \tag{10}$$

Returning to the case where the Hamiltonian is Hermitian, it is convenient to render the two matrices $\widetilde{U}_1$ and $\widetilde{U}_2$ themselves unitary [31, 32]. For this purpose, a 'gauge factor' b is chosen such that the unitary counterparts of $\widetilde{U}_1$ and $\widetilde{U}_2$ are defined via $U_1 = \widetilde{U}_1 b$ and $U_2 = b^{-1}\widetilde{U}_1$. Since $\widetilde{U}_1^\dagger \widetilde{U}_1 = \mathrm{diag}\left(\gamma_1^{(-1)}, \gamma_2\right)$, this would imply that b is the 'Hermitian square-root' of $\mathrm{diag}\left(\gamma_1^{(-1)}, \gamma_2\right)$. This 'Hermitian square-root' is defined by the relation $(b^{(-1)})^\dagger b^{(-1)} = \mathrm{diag}\left(\gamma_1^{(-1)}, \gamma_2\right)$. Inspection of the power series expansion of $\gamma_1^{(\pm\frac{1}{2})} = (\hat{\mathbf{I}} + \mathbf{z}\cdot\mathbf{z}^\dagger)^{(\pm\frac{1}{2})}$ and $\gamma_2^{(\pm\frac{1}{2})} = (\hat{\mathbf{I}} + \mathbf{z}^\dagger\cdot\mathbf{z})^{(\pm\frac{1}{2})}$ shows that since each term in the expansion is Hermitian, matrices $\gamma_1^{\pm\frac{1}{2}}$ and $\gamma_2^{\pm\frac{1}{2}}$ are Hermitian and have non-negative eigenvalues. Because of this, it is sufficient to define b as the inverse square root via $b^{(-2)} = \mathrm{diag}\left(\gamma_1^{(-1)}, \gamma_2\right)$.

Furthermore, $H_{\mathtt{eff}}$ in equation (5) is Hermitian for the unitary counterpart U_1. The upper diagonal block of this Hermitian Hamiltonian accompanying the decomposition $U = U_1 U_2$ is given by

$$\frac{\mathrm{i}}{2}\left[\frac{\mathrm{d}\left(\gamma_1^{-\frac{1}{2}}\right)}{\mathrm{d}t}, \gamma_1^{\frac{1}{2}}\right] + \frac{1}{2}\left(\gamma_1^{-\frac{1}{2}}(\widetilde{\mathbf{H}}^{(N-n)} - \mathbf{z}\mathbf{V}^\dagger)\gamma_1^{\frac{1}{2}} + \mathrm{H.c.}\right), \tag{11}$$

where [,] represents the commutator and H.c. stands for the Hermitian conjugate. The lower diagonal block is similarly given by

$$\frac{\mathrm{i}}{2}\left[\frac{\mathrm{d}\left(\gamma_2^{-\frac{1}{2}}\right)}{\mathrm{d}t}, \gamma_2^{\frac{1}{2}}\right] + \frac{1}{2}\left(\gamma_2^{-\frac{1}{2}}(\widetilde{\mathbf{H}}^{(n)} + \mathbf{z}^\dagger\mathbf{V})\gamma_2^{\frac{1}{2}} + \mathrm{H.c.}\right). \tag{12}$$

For $N = 3$, $n = 1$, these diagonal blocks define an $SU(2)$ and a $U(1)$ Hamiltonian, and $\mathbf{z}$ is a pair of complex numbers. The $SU(2)$ Hamiltonian is in turn rendered in terms of its fiber bundle in figure 1 and the $U(1)$ Hamiltonian corresponds to a phase. Together, they describe a four-dimensional fiber for $SU(3)$ over the base manifold, also four dimensional, of $\mathbf{z}$.

Alternatively, $SU(3)$ problems may be conveniently seen as a part of $SU(4)$ problems, making contact with two-qubit systems that are extensively studied. In this case, for $N = 4$, $n = 2$, these diagonal blocks define two $SU(2)$ Hamiltonians and $\mathbf{z}$ is a 2×2 matrix representable in terms of Pauli spinors. Generally, it is eight dimensional while the fiber has seven dimensions (two $SU(2)$ and a mutual phase) but for the $SU(3)$ subgroup of $SU(4)$, both the base and manifold again reduce to four dimensions each. With $\mathbf{z}$ being a pair of complex numbers, the non-trivial part of geometrizing $SU(3)$ is thereby reduced to describing this four-dimensional manifold. Exploring this for the $N = 3, n = 1$ decomposition will be the content of the following section whereas the appendix gives the alternative $SU(4)$ rendering.

3. Geometry of general $SU(3)$ time-evolution operator

A general time-dependent three-level Hamiltonian may be written in terms of eight linearly independent operators of a three-level system. Such a Hamiltonian can also be written in terms of a subgroup of 15 operators of a four-level system. Before the time-evolution operator is presented in the $SU(3)$ basis in terms of a $N = 3, n = 1$ decomposition, we will note that it can be rendered in a few alternative ways.

First, a general time-dependent four-level Hamiltonian may be written as $H(t) = \sum_i c_i \mathbf{O}_i$. Here c_i are time-dependent and $\mathbf{O}_i$ are the unit matrix and 15 linearly independent operators of a four-level system that may be chosen in a variety of matrix representations. One choice used in particle physics are the so-called Greiner matrices [21–24, 38]. Another choice consists of using $\vec{\sigma}$, $\vec{\tau}$, $\vec{\sigma}\otimes\vec{\tau}$ and the 4×4 unit matrix. Such a choice was discussed in [25, 26] and will

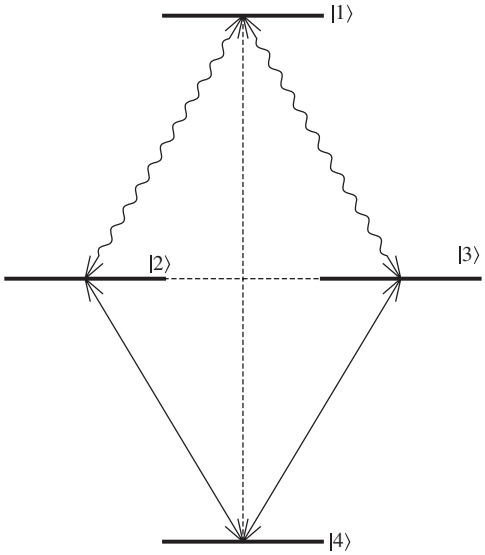

Figure 2. Levels $|2\rangle$ and $|3\rangle$ couple equally to $|1\rangle$ and to $|4\rangle$, which are themselves coupled. The three complex coupling matrix elements and two energy positions define such an $SU(3)$ system.

be used throughout this paper. As it stands, the above Hamiltonian describes a general four-level atom with four energies and six complex couplings. Note that only the three differences in energies are important. Restricting the 15 coefficients c_i to a smaller number allows this Hamiltonian to describe various physical Hamiltonians, forming different subalgebras of the $SU(4)$ algebra [25]. For example, if two of the six complex couplings are zero (levels 1 and 4 and levels 2 and 3 of a four-level atom not coupled), then the Hamiltonian may be recast such that the operators involved belong to an $so(5)$ subalgebra [25]. On the other hand, if levels 2 and 3 are degenerate and level 4 is uncoupled from the rest, then the problem may be recast in terms of only eight operators belonging to the $SU(3)$ subalgebra of $SU(4)$. This is illustrated in figure 2 and is one of the systems of interest in this paper.

Alternatively, after one arrives at the linear equation for the $N = 4, n = 2$ decomposition, one can represent the resulting vector in terms of six homogeneous coordinates. This is the so-called Plücker coordinate representation for the $SU(3)$ Hamiltonian. These coordinates as well as the alternative derivation are presented in the appendix. The $N = 3, n = 1$ decomposition will be the content of the rest of this section.

Consider the Hamiltonian in the basis of the Gell–Mann lambda matrices [39] $H(t) = \sum_i a_i \boldsymbol{\lambda}_i$. The $N = 3, n = 1$ decomposition consists of writing the time-evolution operator in terms of a product of two matrices $U = \widetilde{U}_1 \widetilde{U}_2$ where $\widetilde{U}_1$ is composed of a (2×1)-dimensional $\mathbf{z}$, as explained in section 2. The equation that governs the evolution of $\mathbf{z}$, equation (6), can be written in this case as

$$\dot{z}_\mu = -\mathrm{i}V_\mu - \mathrm{i}F_{\mu\nu}z_\nu + \mathrm{i}V_\nu^* z_\nu z_\mu; \qquad \mu, \nu = 1, 2. \tag{13}$$

Here, the symbols used in defining $\dot{\mathbf{z}}$ are defined as $V = (a_4 - \mathrm{i}a_5, a_6 - \mathrm{i}a_7)$ and

$$F = \begin{pmatrix} a_3 + \sqrt{3}a_8 & a_1 - \mathrm{i}a_2 \\ a_1 + \mathrm{i}a_2 & -a_3 + \sqrt{3}a_8 \end{pmatrix}.$$

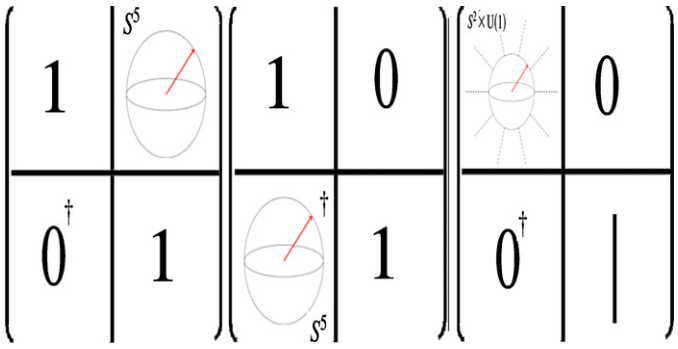

Figure 3. The base and fiber for the $SU(3)$ group. The first two factors give the base manifold, an S^5 sphere with a phase arbitrariness defined in the text. The fiber, described by the third matrix, is composed of a Bloch sphere and a phase associated with each of its points, and the second an extra phase represented by a vertical line in the lower diagonal block.

Using the transformation equations $m_{1,2} = -z_{1,2}(D\,\mathrm{e}^{\mathrm{i}\phi})^{-1}$, $m_3 = (D\,\mathrm{e}^{\mathrm{i}\phi})^{-1}$ and $|m_1|^2 + |m_2|^2 + |m_3|^2 = 1$ leads to the evolution equation for $\vec{m} = (m_{1r}, m_{2r}, m_{3r}, m_{1i}, m_{2i}, m_{3i})^T$:

$$\dot{\vec{m}} = \begin{pmatrix} 0 & -a_2 & a_5 & a_3+\sqrt{3}a_8 & a_1 & -a_4 \\ a_2 & 0 & a_7 & a_1 & -a_3+\sqrt{3}a_8 & -a_6 \\ -a_5 & -a_7 & 0 & -a_4 & -a_6 & 0 \\ -a_3-\sqrt{3}a_8 & -a_1 & a_4 & 0 & -a_2 & a_5 \\ -a_1 & a_3-\sqrt{3}a_8 & a_6 & a_2 & 0 & a_7 \\ a_4 & a_6 & 0 & -a_5 & -a_7 & 0 \end{pmatrix} \vec{m}, \tag{14}$$

which describes the rotation of a unit vector in a six-dimensional space of the real and imaginary parts of $\vec{m}$ defined by $m_\mu = m_{\mu r} + \mathrm{i}m_{\mu i}$. In the above equations, $D = (1 + |z_1|^2 + |z_2|^2)^{1/2}$ and $\mathrm{i}\dot{\phi} = \mathrm{i}(V_\nu^* z_\nu + V_\nu z_\nu^*)$. The phase ϕ is real and determined only up to an additive constant. Since the real and imaginary parts of m_3 are not independently defined, the geometrical description of the base manifold for the $N = 3, n = 1$ decomposition may be thought of as a point on the surface of a constrained six-dimensional unit sphere.

The two constraints, namely $|m_1|^2 + |m_2|^2 + |m_3|^2 = 1$ and the 'phase arbitrariness' of ϕ, reduce the six-dimensional manifold of the three-dimensional complex vector $\vec{m}$ to a four-dimensional manifold in agreement with there being only four independent parameters in $\mathbf{z}$. The first condition defines the base as a vector on an S^5 sphere while the phase arbitrariness serves as an additional constraint. The fiber, on the other hand, is an $SU(2)$ block, evolving as a vector on the S^2 Poincare-like sphere with a phase at each point, and a $U(1)$ block that amounts to an extra phase. This is presented schematically in figure 3, as the product of three matrices of the evolution operator.

The alternative $N = 4$, $n = 2$ decomposition in the appendix yields the equation of motion for $m_\mu = -z_\mu/D\mathrm{e}^{\mathrm{i}\phi}$ in equation (A.11). Following equations (11) and (12), we see that for this case, the two remaining blocks of the time-evolution operator, namely $\widetilde{U}^{(4-2)}$ and $\widetilde{U}^{(2)}$, can be transformed into unitary matrices for $SU(2)$. The fiber evolves as vectors on two identical S^2 Bloch spheres with a mutual phase, whose evolution is coupled to the base that evolves as a vector on an S^5 sphere. This is illustrated in figure 4.

Either decomposition can be used to study various physical processes as will be discussed in the following section.

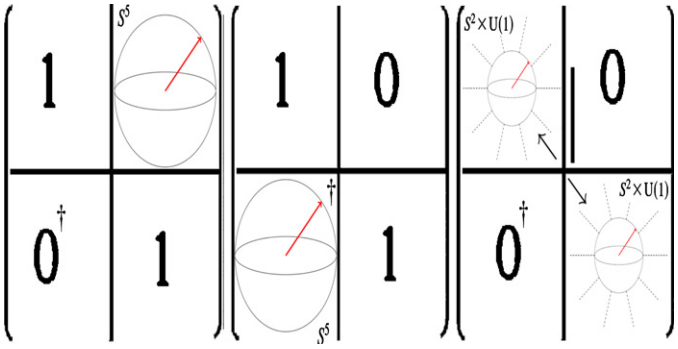

Figure 4. The base and fiber for the $SU(3)$ group via the $N = 4$, $n = 2$ decomposition. The base again is given by an S^5 sphere as in figure 3. The fiber is composed of two identical $SU(2)$ Bloch spheres plus phase, and an extra mutual phase between them. The four parameters each of base and fiber again account for all eight parameters of $SU(3)$.

4. Applications

It is often desirable to control the time evolution of quantum states to manipulate an input state into a desirable output state. In [40, 41], the authors considered a Hamiltonian of form $\mathbf{H}_0 - \mu\mathcal{E}(t)$, where $\mathbf{H}_0$ is a free-field Hamiltonian and $\mu\mathcal{E}(t)$ is a control field. To illustrate the 'Hamiltonian encoding' scheme to control quantum systems, the authors considered a three-level system and studied stimulated Raman adiabatic passage (STIRAP), an atomic coherence effect that employs interference between quantum states to transfer population completely from a given initial state to a specific final state. This is done through a 'counterintuitive' pulse sequence. Consider the Hamiltonian

$$\mathbf{H}(t) = \begin{pmatrix} 0 & G_1(t) & 0 \\ G_1(t) & 2\Delta & G_2(t) \\ 0 & G_2(t) & 0 \end{pmatrix}. \tag{15}$$

Here $G_{1,2}(t) = 2.5\exp[-(t - t_{1,2})^2/\tau^2]$ and $\Delta = 0.1$. The initial population is in the upper state. For $t_1 = \tau$, $t_2 = 0$ and $\tau = 3$, it is seen that the two empty states are coupled first via $G_2(t)$ and then the levels $|1\rangle$ and $|2\rangle$ are coupled through G_1. The dynamics of the populations reveal complete population transfer. A complete solution as per section 3 was constructed for this model, and the results are presented in figure 5 in total agreement with the results of [40].

Quantum control can also be achieved by understanding the nature of tunneling. The famous Landau–Zener formula [5–7] predicts the transition probability of the ground state of a two-level system when the energy levels adiabatically undergo a crossing. The study of level crossings has since been extended to multi-level systems. For example, in [42], the authors considered a three-level atom to study population trapping by manipulating the phase acquired as a three-level system evolves under the influence of frequency modulated fields [43]. Such a frequency modulated field is given by

$$\mathbf{E}(t) = \mathbf{E}_1 \mathrm{e}^{-\mathrm{i}[\omega_1 t + \varphi_1(t)]} + \mathbf{E}_2 \mathrm{e}^{-\mathrm{i}[\omega_2 t + \varphi_2(t)]} + \text{c.c.} \tag{16}$$

$$\varphi_i(t) = M_i \sin \Omega_i t. \tag{17}$$

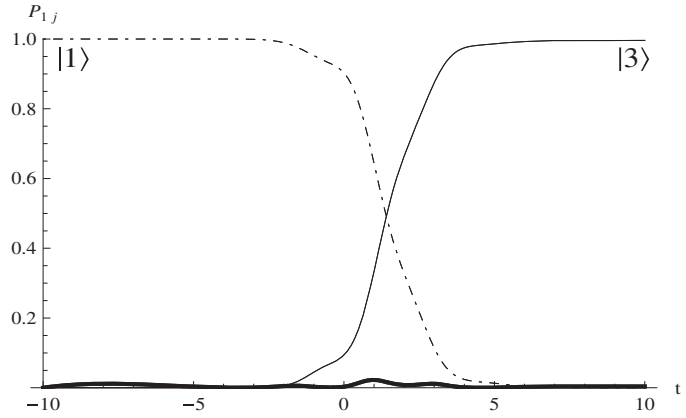

Figure 5. Population $P_{1j} = |\langle 1|j\rangle|^2$ plotted as a function of time. The initial population in state $|1\rangle$ is completely transferred to $|3\rangle$. Both the unitary integration solution and the direct numerical solution [40] are plotted and they coincide at all times.

Here, c.c. stands for the complex conjugation. The phase $\varphi_i(t)$ in the exponent can be written in terms of Bessel functions as [44]

$$e^{M_j \sin \Omega_j t} = \sum_{k=-\infty}^{\infty} J_k(M_j)\, e^{ik\Omega_j t}. \tag{18}$$

For large values of Ω_j, the leading contribution for slow-time scales would come from $J_0(M_j)$. Hence, for large Ω_j, the interaction Hamiltonian can be written as

$$\mathbf{H}_{\text{int}}(t) = -\mathbf{d} \cdot (\mathbf{E}_1 J_0(M_1) + \mathbf{E}_2 J_0(M_2). \tag{19}$$

Hence, for values of $M_{1,2}$ that are zeros of the zeroth-order Bessel functions, the interaction Hamiltonian is zero and population trapping is observed. Under this assumption, consider the full Hamiltonian under the rotating wave approximation,

$$\mathbf{H}(t) = \begin{pmatrix} E_1(t) & G_1(t) & 0 \\ G_1^*(t) & 0 & G_2(t) \\ 0 & G_2^*(t) & E_3(t) \end{pmatrix}.$$

Here, $E_1(t) = \Delta_1 - M_1\Omega_1 \cos(\Omega_1 t + \theta)$ and $E_3(t) = -\Delta_2 + M_2\Omega_2 \cos(\Omega_2 t)$. Results are presented in figure 6, and for the parameter values $\Omega_{1,2} = 1$, $\Delta_1 = -\Delta_2 = 10$, $\theta = 0$ and $G_{1,2} = 6$, demonstrate the phenomenon of population localization discussed in [42].

As a final illustration of the unitary integration technique applied to three-level systems, let us consider the example discussed in [45]. Here, a three-level system is subject to strong fields and the correlation between the scattered light spectrum and the atom dynamics is discussed. The authors consider the Hamiltonian

$$\mathbf{H}(t) = \begin{pmatrix} 0 & 0 & G_1(t) \\ 0 & 0 & G_2(t) \\ G_1^*(t) & G_2^*(t) & 0 \end{pmatrix}. \tag{20}$$

Here, $G_{1,2}(t) = -V_{1,2}\, e^{-i\delta t}$. The time evolution of the states calculated as per our procedure in section 3 is plotted in figure 7 for different values of the parameters. All of these results agree with those given in [45]. Further features of the base and fiber will be presented at the end of the following section.

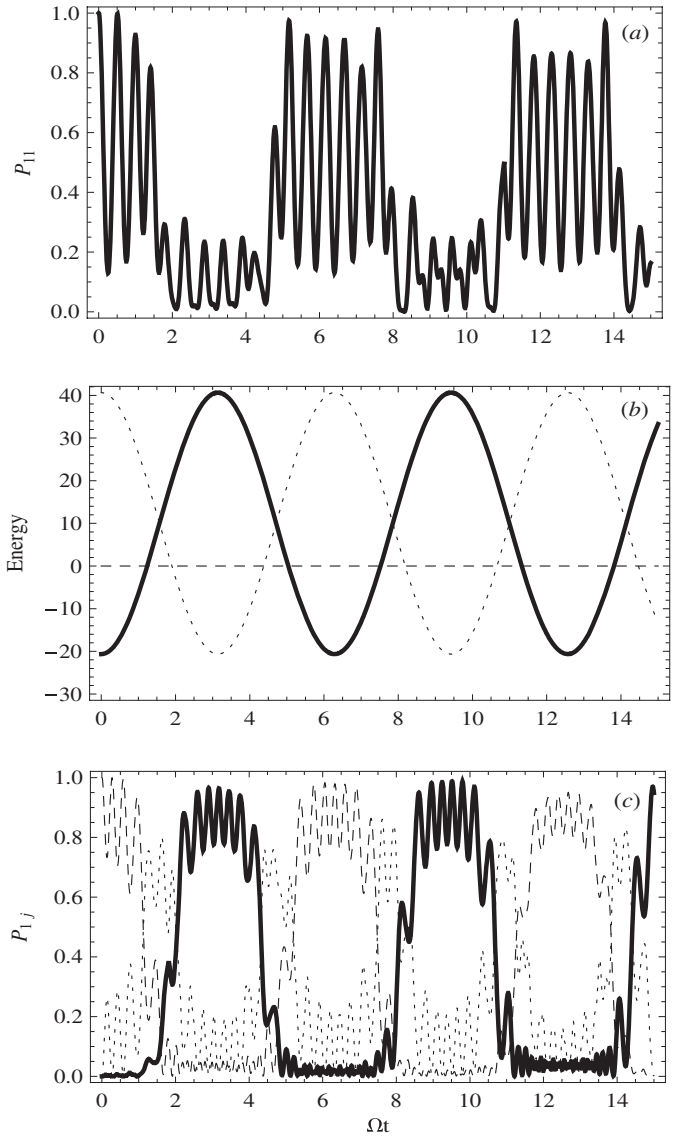

Figure 6. (*a*) For $M_{1,2} = 7$ and the other parameter values given in the text, there is no population trapping observed. (*b*) The energy landscape for $M_{1,2} = 30.6346$ showing energy level crossing. (*c*) Population trapping is observed with $M_{1,2} = 30.6346$ which corresponds to the tenth zero of the zeroth-order Bessel function. Note that the thick line is P_{11} and the thin line corresponds to P_{12}. The results agree completely with [42].

5. Geometric phase for the *SU*(3) group

Many physical systems give rise to a measurable phase that does not depend directly on the dynamical equations that govern the evolution of the system, but depends only on the geometry of the path traversed by vectors characterizing the state of the system. This geometric phase is denoted by γ_g and is given by the integral [46],

$$\gamma_g = \int \mathrm{d}\mathbf{R} \cdot \langle n(\mathbf{R}(t))|\mathrm{i}\nabla_{\mathbf{R}}|n(\mathbf{R}(t))\rangle, \tag{21}$$

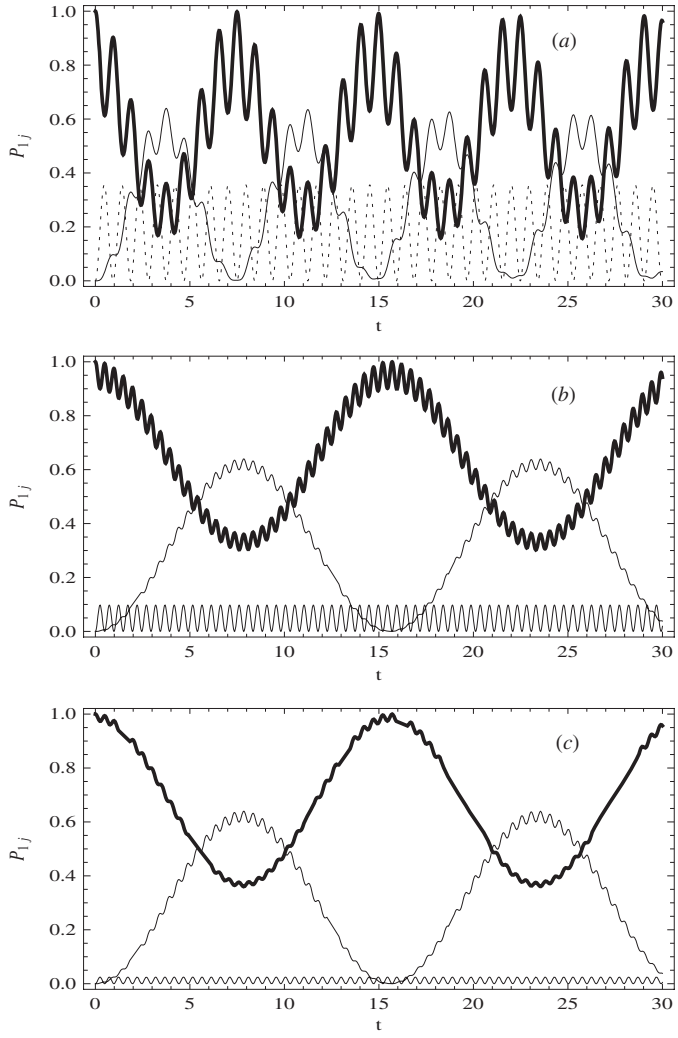

Figure 7. (*a*) Populations $P_{1j} = |\langle 1|j\rangle|^2$ for $\delta = 5$, $V_1 = 2$ and $V_2 = 1$. P_{11} is given by the solid line and P_{12} is given by the thin line. (*b*) Same as (*a*), for $\delta = 12$. Note that P_{13} oscillates close to zero at all times. (*c*) P_{1j} for $\delta = 12$, $V_1 = 1$ and $V_2 = 2$.

where the state evolution is governed by a set of internal coordinates that parameterize the Hamiltonian $\mathbf{R}(t)$, and $\nabla_{\mathbf{R}}$ is the gradient in the space of these internal coordinates. This phase has been generalized to non-cyclic non-adiabatic evolution of quantum systems [35, 36, 47–49]. The purpose of this section is to present this phase in terms of coordinates on the Bloch sphere for two-level systems and extend it to three-level systems.

In two-level systems, the time-evolution operator is described by three parameters as described in section 1. Two of these parameters describe a point on the Bloch sphere. Traversing closed loops on this Bloch sphere returns the quantum system to its initial state as described by the two parameters on the Bloch sphere but not the third parameter of an overall phase. Hence, general closed loops on the Bloch sphere do not correspond to closed loops in the space of the full unitary operator. This discrepancy in the phase between the initial and final states corresponds to the geometric phase given above and amounts to changes along the

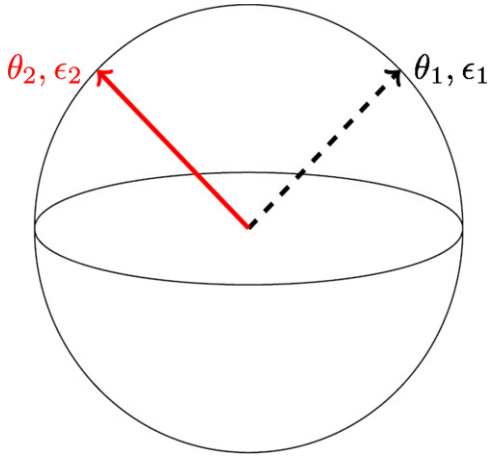

Figure 8. The base manifold U_1 is characterized by two sets of angles $0 \leqslant \theta_i < \pi$, $0 \leqslant \epsilon_i < 2\pi$ which can be represented as two vectors with polar angles (θ_1, ϵ_1) and (θ_2, ϵ_2).

fiber at each point on the sphere. To formalize this, consider U_1, given by equation (3), as unitarized through the matrix b in section 2, which for $N = 2$, $n = 1$ takes the form

$$U_1 = \frac{1}{\sqrt{1 + |\mathbf{z}|^2}} \begin{pmatrix} 1 & \mathbf{z} \\ -\mathbf{z}^* & 1 \end{pmatrix}. \tag{22}$$

By identifying $\cos\frac{\theta}{2} = (1 + |\mathbf{z}|^2)^{-\frac{1}{2}}$ and $\sin\frac{\theta}{2}\mathrm{e}^{-\mathrm{i}\epsilon} = -\mathbf{z}(1 + |\mathbf{z}|^2)^{-\frac{1}{2}}$, we get the usual description of the base manifold in terms of the angles $0 \leqslant \theta < \pi$ and $0 \leqslant \epsilon < 2\pi$ that are associated with the Bloch sphere, namely,

$$U_1 = \begin{pmatrix} \cos\frac{\theta}{2} & -\sin\frac{\theta}{2}\,\mathrm{e}^{-\mathrm{i}\epsilon} \\ \sin\frac{\theta}{2}\,\mathrm{e}^{\mathrm{i}\epsilon} & \cos\frac{\theta}{2} \end{pmatrix}. \tag{23}$$

In terms of the parameters θ and ϵ, the Hamiltonian $H(t) = -\vec{a}\cdot\vec{\sigma}$ is given by

$$H(t) = \begin{pmatrix} -\cos\theta & -\sin\theta\,\mathrm{e}^{-\mathrm{i}\epsilon} \\ -\sin\theta\,\mathrm{e}^{\mathrm{i}\epsilon} & \cos\theta \end{pmatrix}. \tag{24}$$

Equation (5) governing the evolution of the fiber U_2 has two terms. The first term is evaluated as

$$U_1^\dagger H(t) U_1 = \begin{pmatrix} -1 & 0 \\ 0 & 1 \end{pmatrix}, \tag{25}$$

which corresponds to the eigenvalues of the Hamiltonian. To evaluate the second term, consider the case whereby the vector on the Bloch sphere traverses a closed path defined by a constant θ. The second term is then given by

$$U_1^\dagger \frac{\partial U_1}{\partial(-\mathrm{i}\epsilon)} = \begin{pmatrix} -\sin^2\frac{\theta}{2} & -\frac{1}{2}\sin\theta\mathrm{e}^{-\mathrm{i}\epsilon} \\ -\frac{1}{2}\sin\theta\mathrm{e}^{\mathrm{i}\epsilon} & \sin^2\frac{\theta}{2} \end{pmatrix}. \tag{26}$$

Integrating ϵ from 0 to 2π yields

$$\int_0^{2\pi} \mathrm{d}\epsilon U_1^\dagger \frac{\partial U_1}{\partial(-\mathrm{i}\epsilon)} = \begin{pmatrix} \pi(1-\cos\theta) & 0 \\ 0 & -\pi(1-\cos\theta) \end{pmatrix},$$

which is the correct formula for the geometric phase of a two-level system [46].

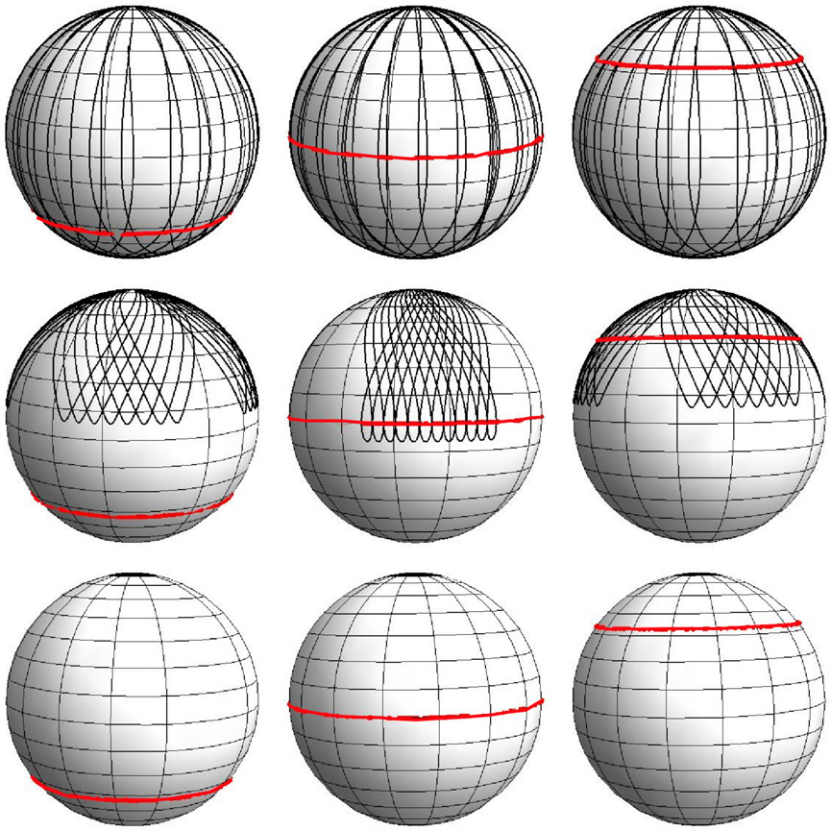

Figure 9. The base manifold corresponding to the results in figure 7 for the three-level system of [45]. For the first column, $V_1 = 1$, $V_2 = 2$. The second column corresponds to $V_1 = 2$, $V_2 = 2$ and the third to $V_1 = 2$, $V_2 = 1$. The rows correspond to $\delta = 1$, $\delta = 5$ and $\delta = 50$. The thin black curve describes (θ_1, ϵ_1) and the thick red curve the set (θ_2, ϵ_2).

To extend this analysis to three-level systems, we consider the $N = 3$, $n = 1$ decomposition. The matrix $U_1 = \widetilde{U}_1 \cdot b$ is now given by

$$U_1 = \begin{pmatrix} \boldsymbol{I}^{(2)} - \frac{1}{D(D+1)}\mathbf{z}\mathbf{z}^\dagger & \frac{\mathbf{z}}{D} \\ -\frac{\mathbf{z}^\dagger}{D} & \frac{1}{D} \end{pmatrix}, \tag{27}$$

where $\mathbf{z}$ is a complex column vector $(z_1, z_2)^T$ and $D = \sqrt{1 + |\mathbf{z}|^2}$. To this effect, we transform $\mathbf{z}$ into polar coordinates: $z_1 = -\tan\frac{\theta_1}{2}\cos\frac{\theta_2}{2}e^{i\epsilon_1}$, $z_2 = -\tan\frac{\theta_1}{2}\sin\frac{\theta_2}{2}e^{i\epsilon_2}$. These transformation equations imply that $D = \sqrt{1 + |\mathbf{z}|^2} = \sec\frac{\theta_1}{2}$. The U_1 matrix is given by

$$U_1 = \begin{pmatrix} 1 - 2\sin^2\frac{\theta_1}{4}\cos^2\frac{\theta_2}{2} & -\sin^2\frac{\theta_1}{4}\sin\theta_2\, e^{i(\epsilon_1-\epsilon_2)} & -\sin\frac{\theta_1}{2}\cos\frac{\theta_2}{2}\, e^{i\epsilon_1} \\ -\sin^2\frac{\theta_1}{4}\sin\theta_2\, e^{-i(\epsilon_1-\epsilon_2)} & 1 - 2\sin^2\frac{\theta_1}{4}\sin^2\frac{\theta_2}{2} & -\sin\frac{\theta_1}{2}\sin\frac{\theta_2}{2}\, e^{i\epsilon_2} \\ \sin\frac{\theta_1}{2}\cos\frac{\theta_2}{2}\, e^{-i\epsilon_1} & \sin\frac{\theta_1}{2}\sin\frac{\theta_2}{2}\, e^{-i\epsilon_2} & \cos\frac{\theta_1}{2} \end{pmatrix}. \tag{28}$$

In the above equation, the range on the polar angles is chosen to be the usual $0 \leqslant \theta_i < \pi$ and $0 \leqslant \epsilon_i < 2\pi$ so that the absolute value of each element of the time-evolution operator is positive [50]. Hence U_1 can be represented as two vectors on a sphere, at angles (θ_1, ϵ_1) and (θ_2, ϵ_2) respectively: figure 8. The transformation equations imply that the vector $\vec{m}$

defined in section 3 is given by $m_1 = \sin\frac{\theta_1}{2}\cos\frac{\theta_2}{2}\,e^{i(\epsilon_1-\phi)}$, $m_2 = \sin\frac{\theta_1}{2}\sin\frac{\theta_2}{2}\,e^{i(\epsilon_2-\phi)}$ and $m_3 = \cos\frac{\theta_2}{2}e^{-i\phi}$. Note that U_1 does not depend on ϕ.

Since the columns of a unitary operator correspond to normalized eigenvectors, we can consider the last column of the matrix above, $|\psi\rangle = \left(-\sin\frac{\theta_1}{2}\cos\frac{\theta_2}{2}\,e^{i\epsilon_1}, -\sin\frac{\theta_1}{2}\sin\frac{\theta_2}{2}\,e^{i\epsilon_2}, \cos\frac{\theta_1}{2}\right)^T$, and evaluate the so-called connection 1-form given by [51]

$$\mathcal{A} = -i\langle\psi|d|\psi\rangle. \tag{29}$$

The Abelian geometric phase, given by $\gamma_g = \int \mathcal{A}$ is evaluated to be

$$\gamma_g = -\frac{1}{2}\int \sin^2\frac{\theta_1}{2}((d\epsilon_1 + d\epsilon_2) + \cos\theta_2(d\epsilon_1 - d\epsilon_2)). \tag{30}$$

If the various angles are relabeled $\epsilon_1 \to -\gamma - \alpha$, $\epsilon_2 \to -\gamma + \alpha$, $\theta_1 \to 2\theta$ and $\theta_2 \to 2\beta$, the formula above agrees with [52] and [50]. The time-evolution operator above can now be used as in the case of $SU(2)$ to evaluate the dynamic contribution $\int U_1^\dagger H(t) U_1$ and the geometric contribution to the time-evolution operator which is given by $-i\int U_1^\dagger dU_1$, where $dU_1 = \frac{dU_1}{d\theta_i}d\theta_i + \frac{dU_1}{d\epsilon_i}d\epsilon_i$, $i = 1, 2$.

This description of the base manifold in terms of (θ_i, ϵ_i) can now be used to describe the dynamics of various physical processes. Figure 9 represents the base manifold corresponding to the results in figure 7. (θ_1, ϵ_1) depend on all the parameters that define the system while (θ_2, ϵ_2) depend only on the ratio V_1/V_2. Also note that the maximum value of ϵ_2, corresponding to the maximum latitude traversed by the black curve, is inversely proportional to δ. Such observations can be used to control the dynamics of this system.

6. Conclusions

The ability to decouple the time dependence of operator equations from the non-commuting nature of the operators is the central feature of unitary integration and also characterizes the Bloch sphere representation for the evolution of a single spin. By doing so, the quantum mechanical evolution is rendered a 'classical' picture of a rotating unit vector. For a two-level atom, the Bloch sphere representation along with a phase completely determines the time-evolution operator. In this paper, we have extended this program to deal with the time-evolution operator belonging to the $SU(3)$ group. This complements the work in [31] for $SU(4)$ Hamiltonians of two-qubit systems. We have also extended the analysis of geometric phase to three-level systems by providing an explicit coordinate representation for the $SU(3)$ time-evolution operator.

Appendix. Alternative derivations for a general $SU(3)$ Hamiltonian.

Consider a three-level Hamiltonian written in terms of the Gell–Mann matrices [39] as $H(t) = \sum_{i=1}^{8} a_i \boldsymbol{\lambda}_i$. To exploit the fact that this Hamiltonian is a subgroup of four-level problems, it is represented in terms of the O matrices [25, 26] as

$$\begin{aligned} 2\frac{a_8}{\sqrt{3}}\mathbf{O}_2 + \left(a_3 - \frac{a_8}{\sqrt{3}}\right)\mathbf{O}_3 + \left(2a_3 + 2\frac{a_8}{\sqrt{3}}\right)\mathbf{O}_4 + a_4\mathbf{O}_5 + a_5\mathbf{O}_6 + 2a_4\mathbf{O}_7 + 2a_5\mathbf{O}_8 \\ + a_1\mathbf{O}_9 + a_2\mathbf{O}_{10} + 2a_1\mathbf{O}_{11} + 2a_2\mathbf{O}_{12} \\ + 2a_6\mathbf{O}_{13} + 2a_6\mathbf{O}_{14} - 2a_7\mathbf{O}_{15} + 2a_7\mathbf{O}_{16}. \end{aligned} \tag{A.1}$$

This embeds the Hamiltonian $H(t) = \sum_i a_i\boldsymbol{\lambda}_i$ as a 4×4 matrix with zeros along the last row and column. In such a representation, the various entries of the Hamiltonian equation (2) are

given by

$$H^{(4-2)} = \tfrac{1}{\sqrt{3}}a_8\mathbf{I}^{(2)} + a_1\boldsymbol{\sigma}_1 + a_2\boldsymbol{\sigma}_2 + a_3\boldsymbol{\sigma}_3, \tag{A.2}$$

$$H^{(2)} = -\tfrac{1}{\sqrt{3}}a_8\mathbf{I}^{(2)} - \tfrac{1}{\sqrt{3}}a_8\boldsymbol{\sigma}_1, \tag{A.3}$$

$$\mathbf{V} = \tfrac{1}{2}(a_4 - \mathrm{i}a_5)\mathbf{I}^{(2)} + \tfrac{1}{2}(a_6 - \mathrm{i}a_7)\boldsymbol{\sigma}_1 - \mathrm{i}\tfrac{1}{2}(a_6 - \mathrm{i}a_7)\boldsymbol{\sigma}_2 + \tfrac{1}{2}(a_4 - \mathrm{i}a_5)\boldsymbol{\sigma}_3. \tag{A.4}$$

Writing $\mathbf{z}$ in the standard Clifford basis as $\mathbf{z} = \frac{1}{2}z_4\mathbf{I}^{(2)} - \frac{\mathrm{i}}{2}\sum_i z_i\boldsymbol{\sigma}_i$, it follows from equation (6) that $z_1 = \mathrm{i}z_2$ and $z_3 = \mathrm{i}z_4$ and the equation reduces precisely to equation (13). The geometry described in section 3 can thus be derived from either of these decompositions of the time-evolution operator.

The $SU(3)$ subgroup in equation (A.1) is one among many $SU(3)$ subgroups embedded in $SU(4)$. Another choice corresponds to the Dzyaloshinskii–Moriya interaction Hamiltonian [12, 13] and is also of interest because the 4×4 matrices now do not have a trivial row and column of zeros. In the two-spin basis, this Hamiltonian is given by

$$\begin{aligned} H(t) = \sum_i c_i\mathbf{O}_i &= a_1(\mathbf{O}_2 + \mathbf{O}_3) + 2a_2(\mathbf{O}_{15} + \mathbf{O}_{16}) + 2a_3(\mathbf{O}_{14} - \mathbf{O}_{13}) + 2a_4(\mathbf{O}_7 + \mathbf{O}_{11}) \\ &\quad + a_5(\mathbf{O}_6 + \mathbf{O}_{10}) + a_6(\mathbf{O}_5 + \mathbf{O}_9) + 2a_7(\mathbf{O}_8 + \mathbf{O}_{12}) \\ &\quad + \frac{2a_8}{\sqrt{3}}(2\mathbf{O}_4 - \mathbf{O}_{13} - \mathbf{O}_{14}). \end{aligned} \tag{A.5}$$

The correspondence between the coefficients in terms of $\mathbf{O}$ and in terms of the $\boldsymbol{\lambda}$ matrices is: $c_1 = 0$, $c_2 = a_1$, $c_3 = a_1$, $c_4 = 4a_8/\sqrt{3}$, $c_5 = a_6$, $c_6 = a_5$, $c_7 = 2a_4$, $c_8 = 2a_7$, $c_9 = a_6$, $c_{10} = a_5$, $c_{11} = 2a_4$, $c_{12} = 2a_7$, $c_{13} = -2a_3 - 2a_8/\sqrt{3}$, $c_{14} = 2a_3 - 2a_8/\sqrt{3}$, $c_{15} = 2a_2$ and $c_{16} = 2a_2$. Relabeling of the states $1 \to 2$, $2 \to 3$, $3 \to 4$ and $4 \to 1$ expresses the Hamiltonian as

$$H^{(4-2)} = \tfrac{1}{\sqrt{3}}a_8\mathbf{I}^{(2)} - a_3\boldsymbol{\sigma}_1 - a_2\boldsymbol{\sigma}_2 - a_1\boldsymbol{\sigma}_3, \tag{A.6}$$

$$H^{(2)} = -\tfrac{1}{\sqrt{3}}a_8\mathbf{I}^{(2)} - \tfrac{1}{\sqrt{3}}a_8\boldsymbol{\sigma}_1, \tag{A.7}$$

$$\mathbf{V} = \tfrac{1}{2}(a_6 - \mathrm{i}a_7)\mathbf{I}^{(2)} + \tfrac{1}{2}(a_6 - \mathrm{i}a_7)\boldsymbol{\sigma}_1 - \tfrac{1}{2}(a_5 + \mathrm{i}a_4)\boldsymbol{\sigma}_2 - \tfrac{1}{2}(a_4 - \mathrm{i}a_5)\boldsymbol{\sigma}_3. \tag{A.8}$$

If $\mathbf{z}$ is written in terms of the standard Clifford basis $(\hat{\mathbf{I}}, -\mathrm{i}\vec{\boldsymbol{\sigma}})$ as $\mathbf{z} = \frac{1}{2}z_4\mathbf{I}^{(2)} - \frac{\mathrm{i}}{2}\sum_{i=1}^{3} z_i\boldsymbol{\sigma}_i$, it follows from equation (6) that $z_1 = \mathrm{i}z_4$ and $z_2 = \mathrm{i}z_3$. This is consistent with the parameter count that since the inhomogeneity $\mathbf{V}$ has only two free complex parameters (namely $V_1 = a_6 - \mathrm{i}a_7$ and $V_2 = a_4 - \mathrm{i}a_5$), the complex $\mathbf{z}$ matrix should be composed only of two independent complex parameters, z_1 and z_2. With the above analysis, equation (6) becomes for the pair of complex numbers

$$\tfrac{1}{2}\dot{z}_\mu = \tfrac{1}{2}X_\mu - \mathrm{i}F_{\mu\nu}z_\nu + 2G_\nu z_\nu z_\mu; \qquad \mu, \nu = 1, 2. \tag{A.9}$$

Here $X = (V_1/2, -\mathrm{i}V_2/2)$, $G = \left(2V_1^*, 2\mathrm{i}V_2^*\right)$ and

$$-\mathrm{i}F = \begin{pmatrix} \mathrm{i}a_3 - \sqrt{3}\mathrm{i}a_8 & a_1 + \mathrm{i}a_2 \\ -a_1 + \mathrm{i}a_2 & -\mathrm{i}a_3 - \sqrt{3}\mathrm{i}a_8 \end{pmatrix}.$$

Paralleling the technique employed to solve an $SO(5)$ Hamiltonian in [31, 32], we transform $\mathbf{z}$ into a complex vector $\vec{m}$: $m_\mu = \frac{-2z_\mu e^{\mathrm{i}\phi}}{D}$ and $m_3 = \frac{e^{\mathrm{i}\phi}}{D}$ such that $|m_1|^2 + |m_2|^2 + |m_3|^2 = 1$, with $D = (1 + 4(|z_1|^2 + |z_2|^2))^{1/2}$. This leads to the new set of evolution equations

$$\dot{\vec{m}} = \begin{pmatrix} \mathrm{i}a_3 - \sqrt{3}\mathrm{i}a_8 & a_1 + \mathrm{i}a_2 & -a_6 + \mathrm{i}a_7 \\ -a_1 + \mathrm{i}a_2 & -\mathrm{i}a_3 - \sqrt{3}\mathrm{i}a_8 & a_5 + \mathrm{i}a_4 \\ a_6 + \mathrm{i}a_7 & -a_5 + \mathrm{i}a_4 & 0 \end{pmatrix}\vec{m}. \tag{A.10}$$

This can be written as an equation describing the rotation of the real and imaginary components of the vector $\vec{m} = (m_{1r}, m_{2r}, m_{3r}, m_{1i}, m_{2i}, m_{3i})^T$,

$$\dot{\vec{m}} = \begin{pmatrix} 0 & a_1 & -a_6 & -a_3+\sqrt{3}a_8 & -a_2 & -a_7 \\ -a_1 & 0 & a_5 & -a_2 & a_3+\sqrt{3}a_8 & -a_4 \\ a_6 & -a_5 & 0 & -a_7 & -a_4 & 0 \\ a_3-\sqrt{3}a_8 & a_2 & a_7 & 0 & a_1 & -a_6 \\ a_2 & -a_3-\sqrt{3}a_8 & a_4 & -a_1 & 0 & a_5 \\ a_7 & a_4 & 0 & a_6 & -a_5 & 0 \end{pmatrix} \vec{m}. \tag{A.11}$$

Here, the coefficients c_i are written in terms of the coefficients a_i, whose correspondence was given earlier in this section. Also note that $m_\mu = m_{\mu r} + \mathrm{i}m_{\mu i}$, $D = (1+|z_1|^2+|z_2|^2)^{\frac{1}{2}}$ and $\dot{\phi} = (V_\nu^* z_\nu + V_\nu z_\nu^*)$. Simplifying this leads to the equation $\mathrm{i}\dot{\phi} = -2\big(X_\mu z_\mu^* - X_\mu^* z_\mu\big)$ for the evolution of ϕ which is clearly real but determined only to within a constant. A little algebra yields for the effective Hamiltonian given by equation (11),

$$H^{(4-2)} - \frac{1}{(D+1)}(\mathbf{z}\mathbf{V}^\dagger + \mathbf{V}\mathbf{z}^\dagger) - \frac{1}{2(D+1)^2}(\mathbf{z}\mathbf{V}^\dagger\mathbf{z}\mathbf{z}^\dagger + \mathbf{z}\mathbf{z}^\dagger\mathbf{V}\mathbf{z}^\dagger),$$

and for the effective Hamiltonian given by equation (12), the expression $H^{(2)} + (\mathbf{z}^\dagger\mathbf{V} + \mathbf{V}^\dagger\mathbf{z})/2$.

Another representation of the $SU(3)$ subgroup of $SU(4)$ Hamiltonians is given by the so-called Plücker coordinate representation of the $SU(4)$ group discussed in [31, 32]. For an arbitrary $SU(4)$ matrix, the Plücker coordinates are defined as a set of six parameters $(P_{12}, P_{13}, P_{14}, P_{23}, P_{24}, P_{34})$ such that $P_{12}P_{34} - P_{13}P_{24} + P_{14}P_{23} = 0$ and $\sum |P_{ij}|^2 = 1$. They can be written in terms of the unit vector $\vec{m}$ and are given by

$$\begin{pmatrix} P_{12} \\ P_{13} \\ P_{14} \\ P_{23} \\ P_{24} \\ P_{34} \end{pmatrix} = \frac{1}{2}\begin{pmatrix} \mathrm{i}m_6 - m_5 \\ \mathrm{i}m_1 + m_2 \\ -\mathrm{i}m_3 + m_4 \\ -\mathrm{i}m_3 - m_4 \\ -\mathrm{i}m_1 + m_2 \\ \mathrm{i}m_6 + m_5 \end{pmatrix}. \tag{A.12}$$

The linear equation of motion for $\vec{m}$ translates into an evolution equation for $\mathbf{P} = (P_{12}, -P_{13}, P_{14}, P_{23}, P_{24}, P_{34})$ of the form $\mathrm{i}\dot{\mathbf{P}} = \mathbf{H}_P\mathbf{P}$. Here, $\mathbf{H}_P$ is given by

$$\mathbf{H}_P = \begin{pmatrix} \mathbf{H}_{P1} & \mathbf{V}_P \\ \mathbf{V}_P^\dagger & \mathbf{H}_{P2} \end{pmatrix}, \tag{A.13}$$

where

$$\mathbf{H}_{P1} = \begin{pmatrix} 2a_8/\sqrt{3} & a_{64-} + \mathrm{i}a_{75-} & a_{64-} + \mathrm{i}a_{75-} \\ a_{64-} - \mathrm{i}a_{75-} & -a_1 & a_8/\sqrt{3} \\ a_{64-} - \mathrm{i}a_{75-} & a_8/\sqrt{3} & -a_1 \end{pmatrix},$$

$$\mathbf{H}_{P2} = \begin{pmatrix} a_1 & -a_8/\sqrt{3} & -a_{64-} - \mathrm{i}a_{75-} \\ -a_8/\sqrt{3} & a_1 & -a_{64-} - \mathrm{i}a_{75-} \\ -a_{64-} + \mathrm{i}a_{75-} & -a_{64-} + \mathrm{i}a_{75-} & -2a_8/\sqrt{3} \end{pmatrix},$$

$$\mathbf{V}_P = \begin{pmatrix} -a_{64+} - \mathrm{i}a_{75+} & a_{64+} + \mathrm{i}a_{75+} & 0 \\ a_{32-} & 0 & -a_{64+} - \mathrm{i}a_{75+} \\ 0 & -a_{32-} & a_{64+} - \mathrm{i}a_{75+} \end{pmatrix}.$$

In the above equations, $a_{ij\pm}$ denotes $a_i \pm a_j$.

References

[1] Scully M O and Zubairy M S 1996 *Quantum Optics* (Cambridge: Cambridge University Press) (section 7.3)
[2] Oreg J, Hioe F T and Eberly J H 1984 *Phys. Rev.* A **29** 690
[3] Kuklinski J R, Gaubatz U, Hioe F T and Bargmann K 1989 *Phys. Rev.* A **40** 6741
[4] Chelkowski S and Gibson S 1995 *Phys. Rev.* A **52** R3417
[5] Landau L D 1932 *Phys. Z. Sowjetunion* **2** 46
[6] Zener C 1932 *Proc. R. Soc.* A **137** 696
[7] Stückelberg E C G 1932 *Helv. Phys. Acta* **5** 369
[8] Ivanov S S and Vitanov N V 2008 *Phys. Rev.* A **77** 023406
[9] Kobayashi M and Maskawa T 1983 *Prog. Theor. Phys.* **49** 652
[10] Bonesteel N E, Stepanenko D and DiVincenzo D P 2001 *Phys. Rev. Lett.* **87** 207901
[11] Kavokin K V 2001 *Phys. Rev.* B **64** 075305
[12] Dzyaloshinskii I 1958 *J. Phys. Chem. Solids* **4** 241
[13] Moriya T 1960 *Phys. Rev.* **120** 91
[14] Chandler D 1987 *Introduction to Modern Statistical Mechanics* (New York: Oxford University Press) (section 5.1)
[15] Gottfried K and Yan T 2004 *Quantum Mechanics: Fundamentals* 2nd edn. (New York: Springer) pp 447–48
[16] Bengtsson I and Zyczkowski K 2006 *Geometry of Quantum States* (Cambridge: Cambridge University Press)
[17] Wei J and Norman E 1963 *J. Math. Phys.* **4** 575
[18] Dattoli G and Torre A 1991 *Riv. Nuovo Cimento* **106** 1247
[19] Mosseri R and Dandoloff R 2001 *J. Phys. A: Math. Gen.* **34** 10243
[20] Tilma T, Byrd M and Sudarshan E C G 2002 *J. Phys. A: Math. Gen.* **35** 10445
[21] Rau A R P 1998 *Phys. Rev. Lett.* **81** 4785
[22] Shadwick B A and Buell W F 1997 *Phys. Rev. Lett.* **79** 5189
[23] Rau A R P and Wendell R A 2002 *Phys. Rev. Lett.* **89** 220405
[24] Rau A R P and Zhao W 2003 *Phys. Rev.* A **68** 052102
[25] Rau A R P, Selvaraj G and Uskov D B 2003 *Phys. Rev.* A **71** 062316
[26] Rau A R P 2000 *Phys. Rev.* A **61** 032301
[27] Zhang J, Vela J, Sastry S and Whaley K B 2003 *Phys. Rev.* A **67** 042313
[28] Hioe F T and Eberly J H 1981 *Phys. Rev. Lett.* **47** 838
[29] Dattoli G, Mari C and Torre A 1992 *Il Nuovo Cimento* **107** 167
[30] Englert B G and Metwally N 2000 *J. Mod. Opt.* **47** 2221
[31] Uskov D B and Rau A R P 2006 *Phys. Rev.* A **78** 022331
[32] Uskov D B and Rau A R P 2006 *Phys. Rev.* A **74** 030304
[33] Klimov A B, Sánchez-Soto L L, de Guise H and Björk G 2004 *J. Phys. A: Math. Gen.* **37** 4097
[34] Ben-Aryeh Y 2003 *Opt. Spectrosc.* **94** 724
[35] Giavarini G and Onofri E 1989 *J. Math. Phys.* **30** 659
[36] Giavarini G and Onofri E 1990 *Int. J. Mod. Phys.* A **5** 4311
[37] Sakurai J J 1994 *Modern Quantum Mechanics* (Reading, MA: Addison-Wesley) (section 2.1)
[38] Greiner W and Müller B 1994 *Quantum Mechanics: Symmetries* 2nd edn. (Berlin: Springer) (section 7.2)
[39] Georgi H 1999 *Lie Algebras in Particle Physics* (Reading, MA: Perseus Books) (section 7.1)
[40] Mitra A, Solá I and Rabitz H 2003 *Phys. Rev.* A **67** 043409
[41] Mitra A, Solá I and Rabitz H 2003 *Phys. Rev.* A **67** 033407
[42] Harshawardhan W and Agarwal G S 1997 *Phys. Rev.* A **55** 2165
[43] Harshawardhan W and Agarwal G S 1997 *Phys. Rev.* A **50** R4465
[44] Abramowitz M and Stegun I A 1972 *Handbook of Mathematical Functions with Formulas, Graphs and Mathematical Tables* (New York: Dover)
[45] Kancheva L, Pushkarov D and Rashev S 1981 *J. Phys. B: At. Mol. Phys.* **14** 573
[46] Berry M V 1984 *Proc. R. Lond.* A **392** 45
[47] Samuel J and Bhandari R 1988 *Phys. Rev. Lett.* **60** 2339
[48] Aharanov Y and Anandan J 1987 *Phys. Rev. Lett.* **58** 1593
[49] Wilczek F and Zee A 1984 *Phys. Rev. Lett.* **52** 2111
[50] Aravind, Mallesh K S and Mukunda N 1997 *J. Phys. A: Math. Gen.* **30** 2417
[51] Bohm A, Mostafazadeh A, Koizumi H, Niu H and Zwanziger Q J 2003 *Geometric Phase in Quantum Systems* (Berlin: Springer)
[52] Byrd M 1999 Geometric phases for three state systems arXiv:quant-ph/9902061v1